



Rapid, ultraviolet-induced, reversibly switchable wettability of superhydrophobic/superhydrophilic surfaces

Yunlu Pan¹, Wenting Kong¹, Bharat Bhushan^{*1,2} and Xuezheng Zhao^{*1}

Full Research Paper

Open Access

Address:

¹Key laboratory of Micro-Systems and Micro-Structures Manufacturing of Ministry of Education and School of Mechatronics Engineering, Harbin Institute of Technology, Xidazhi 92, Harbin, 150001, PR China and ²Nanoprobe Laboratory for Bio- & Nanotechnology and Biomimetics (NLBB), The Ohio State University, 201 W. 19th Avenue, Columbus, OH 43210-1142, USA

Email:

Bharat Bhushan^{*} - bhushan.2@osu.edu; Xuezheng Zhao^{*} - zhaoxz@hit.edu.cn

* Corresponding author

Keywords:

superhydrophilic surfaces; superhydrophobic surfaces; switchable wettability; TiO₂; trimethoxy(alkyl)silane; UV illumination

Beilstein J. Nanotechnol. **2019**, *10*, 866–873.

doi:10.3762/bjnano.10.87

Received: 26 November 2018

Accepted: 08 March 2019

Published: 15 April 2019

Associate Editor: N. Motta

© 2019 Pan et al.; licensee Beilstein-Institut.

License and terms: see end of document.

Abstract

Controllable wettability is important for a wide range of applications, including intelligent switching, self-cleaning and oil/water separation. In this work, rapid switching and extreme wettability changes upon ultraviolet (UV) illumination were investigated. TiO₂ nanoparticles were modified in solutions of trimethoxy(alkyl)silane, and the suspensions were sprayed on glass substrates. For such samples, the water contact angle (WCA) was shown to transition from a superhydrophobic (WCA \approx 165°) to a superhydrophilic (WCA \approx 0°) state within 10 min upon UV illumination and subsequent recovery to superhydrophobicity occurred after heat treatment. It was found that the changes in the trimethoxy(alkyl)silane upon UV illumination can explain the rapid decrease of the WCA from more than 165° to almost 0°. To further investigate the wettability transition, trimethoxy(alkyl)silane and Al₂O₃ nanoparticles (which are not photocatalytic) were mixed and spray-coated onto the glass substrates as the control samples. Then the unrecoverable change of trimethoxy(alkyl)silane under UV illumination can be confirmed. It was found that the presence of trimethoxy(alkyl)silane in the TiO₂–trimethoxy(alkyl)silane coating served to speed up the super-wettability transition time from superhydrophobicity to superhydrophilicity, but also limited the number of wettability recycle times. With this understanding, the effect of the trimethoxy(alkyl)silane concentration on the number of recycle cycles was investigated.

Introduction

Wettability is an important property of solid surfaces governed by surface chemistry and surface topography [1,2] and has found significant applications in various fields [3–8]. Control-

lable wettability that can be enabled through external stimuli, such as illumination, electric fields or heating, can be applied in chemical sensors, smart filtration and separation, and micro-

fluidic devices [9-12]. While controlling wettability through heating is mostly limited to toxic materials, such surfaces cannot be applied in human science [13,14]. Although the application of an electric field is an efficient method to achieve switchable wettability, the range of variation in the wettability is still limited [15,16]. Among the numerous approaches to achieve switchable wettability, UV illumination is highly preferred due to its environmentally friendly, non-contact and convenient manner. TiO₂ nanoparticles are a common photocatalysis material that has attracted attention since it is more sensitive to UV light [17]. The use of a photochemical method to strengthen the interaction between nanoparticles and organic materials is quite common [18,19]. TiO₂ nanoparticles modified with organic materials that have a low surface energy could be used to induce the property of switchable wettability under UV illumination.

In order to be useful for many applications, the ability to rapidly switch the wettability from superhydrophobicity to superhydrophilicity is imperative. Several studies based on TiO₂ have been carried out to prepare surfaces exhibiting reversible wettability [20]. Wang et al. [21] prepared a TiO₂ polycrystalline film which achieved drastic changes in wettability when the water contact angle (WCA) was changed from 72° and 0° under UV illumination, followed by recovery at around 70° after storing in the dark. Jin et al. [22] modified TiO₂ with 7-[4-(trifluoromethoxyphenylazo)phenoxy]pentanoic acid (CF₃AZO) which could reversibly switch between hydrophobic (≈145°) and hydrophilic (≈24°) under UV illumination for about 13 h. Chagas et al. [23] fabricated surfaces that were reversibly wettable by dipping polypropylene surfaces in a suspension of TiO₂ modified with trimethoxypropyl silane. In this work, the wettability transition time from superhydrophobic (WCA ≈ 158°) to superhydrophilic (WCA ≈ 0°) occurred within 120 min of UV illumination.

Although large range wettability switching can be achieved in many ways, the transition from superhydrophobic to superhydrophilic always requires a longer time, ranging from a couple of days to a couple of hours [23-27]. Some studies have been carried out to reduce the wettability transition time. Sawada et al. [28] fabricated surfaces with TiO₂/fluoroalkyl end-capped vinyltrimethoxysilane sol-gel where the WCA changed from about 180° to 108° in under 50 min upon UV illumination and then further reduced to 20° after another 30 min. Thus the total transition time from superhydrophobic to superhydrophilic was about 80 min. Petroffe et al. [29] modified TiO₂ with 11-(4-(phenylazo)phenoxy)undecanoic acid (AzoC11) acid to fabricate a hybrid surface which could achieve a rapid change in wettability properties within 12 min, however the wettability range was only between hydrophobic (≈146°) and hydrophilic

(≈21°). Qing et al. [30] fabricated superhydrophobic TiO₂ nanoparticles with (heptadecafluoro-1,1,2,2-tetradecyl)trimethoxysilane, which not only exhibited reversible wettability from 160° to 0° but also reduced the transition time to 60 min.

By modifying trimethoxy(alkyl)silane, TiO₂-based surfaces can achieve a faster change from superhydrophobic to superhydrophilic. However, the reason of the faster transition process has not explained. Due to the high energy of UV illumination and the photocatalysis effect of TiO₂, the -CF₂-, -CF₃ groups of the modified trimethoxy(alkyl)silane might become photodegraded and the end of the trimethoxy(alkyl)silane would change into -OH groups without reversibility [31,32]. It can then be assumed that the degradation of trimethoxy(alkyl)silane could reduce the transition time from superhydrophobic to superhydrophilic for surfaces modified with TiO₂ nanoparticles and trimethoxy(alkyl)silane.

In this study, to confirm this assumption, a series of experiments were carried out. Surfaces were coated with TiO₂ nanoparticles and non-photosensitive Al₂O₃ nanoparticles as the control groups, respectively. The nanoparticles were modified with a short carbon chain trimethoxy(alkyl)silane, 1H,1H,2H,2H-perfluorooctyl(trimethoxy)silane (PFOS), in different concentrations. The wettability and the chemical bonding of the surfaces were tested upon UV illumination and heating treatments. The results are in agreement with the proposed assumption that the oxidation of the trimethoxy(alkyl)silane could decrease the super-wettability transition time, however the reversibility will be limited due to the irreversible oxidation process. The effect of trimethoxy(alkyl)silane concentration on the number of times the surface can be recycled was also investigated.

Results and Discussion

Characterization of the superhydrophobic coating

The hydrophilic TiO₂ nanoparticles were modified in ethanol solutions of PFOS, and the suspensions were sprayed on glass substrates to make the TiO₂-PFOS samples. With the same method, Al₂O₃-PFOS samples were prepared as control groups. As shown in Figure 1, both TiO₂-PFOS and Al₂O₃-PFOS coated surfaces exhibited excellent superhydrophobicity, and the WCA was measured as about 165° and 171°, respectively. Based on the SEM images shown in Figure 1, two-dimensional micro-nanostructures can be obviously seen on the two kinds of surfaces due to the aggregation of nanoparticles, which can explain the good superhydrophobicity.

The TiO₂ nanoparticles were subjected to chemical bonding as Si-O-Ti with hydrolysing PFOS. The chemical bonding is veri-

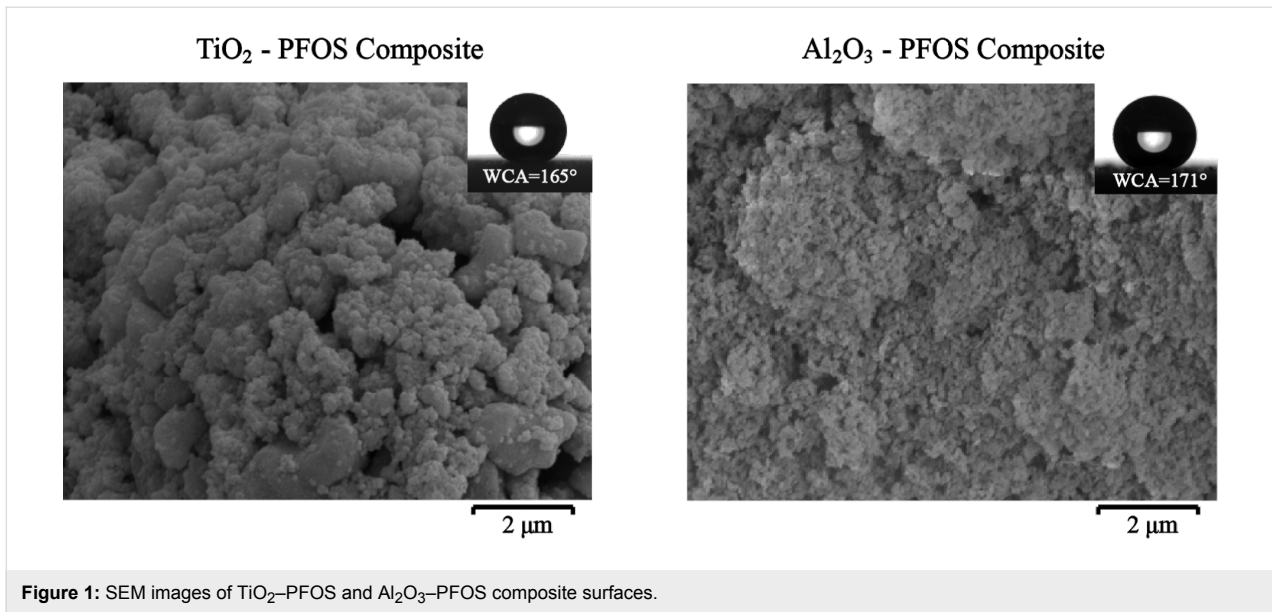


Figure 1: SEM images of TiO_2 -PFOS and Al_2O_3 -PFOS composite surfaces.

fied by the Fourier transfer infrared (FTIR) spectra of TiO_2 and TiO_2 -PFOS coated glass surfaces, as shown in Figure 2. The asymmetric stretching vibration of the Si-O-Ti species was displayed at the absorption peak of 1065 cm^{-1} which further confirmed the dehydration reaction occurred between the hydrolytic PFOS and TiO_2 . Additionally, there were another three peaks at 1157 , 1207 , 1243 cm^{-1} , which correspond to the stretching vibration of $-\text{CF}_2-$ and $-\text{CF}_3$ groups [24,30]. Similarly, the absorption peak of $-\text{CF}_2-$ and $-\text{CF}_3$ groups appeared in the FTIR spectra of Al_2O_3 -PFOS but without the peak at 1065 cm^{-1} , which indicates that there was probably no chemical bonding between Al_2O_3 and PFOS, suggesting the physical adhesion between Al_2O_3 nanoparticles and PFOS.

Wettability switching by UV illumination and heating

Both TiO_2 -PFOS coated surfaces and Al_2O_3 -PFOS coated surfaces were directly illuminated under a UV lamp at a working distance of 10 mm, and the WCAs were recorded every 5 min. The TiO_2 -PFOS coated surface transitioned from superhydrophobicity to superhydrophilicity after only 10 min of UV exposure, while it took 90 min for Al_2O_3 -PFOS surfaces to transition. Then the samples were heated at $150\text{ }^\circ\text{C}$ for 90 min, the property of superhydrophobicity was recovered for the TiO_2 -PFOS coated surface, while the Al_2O_3 -PFOS coated surface remained superhydrophilic. A transition time of 10 min from superhydrophobic to superhydrophilic is much faster than

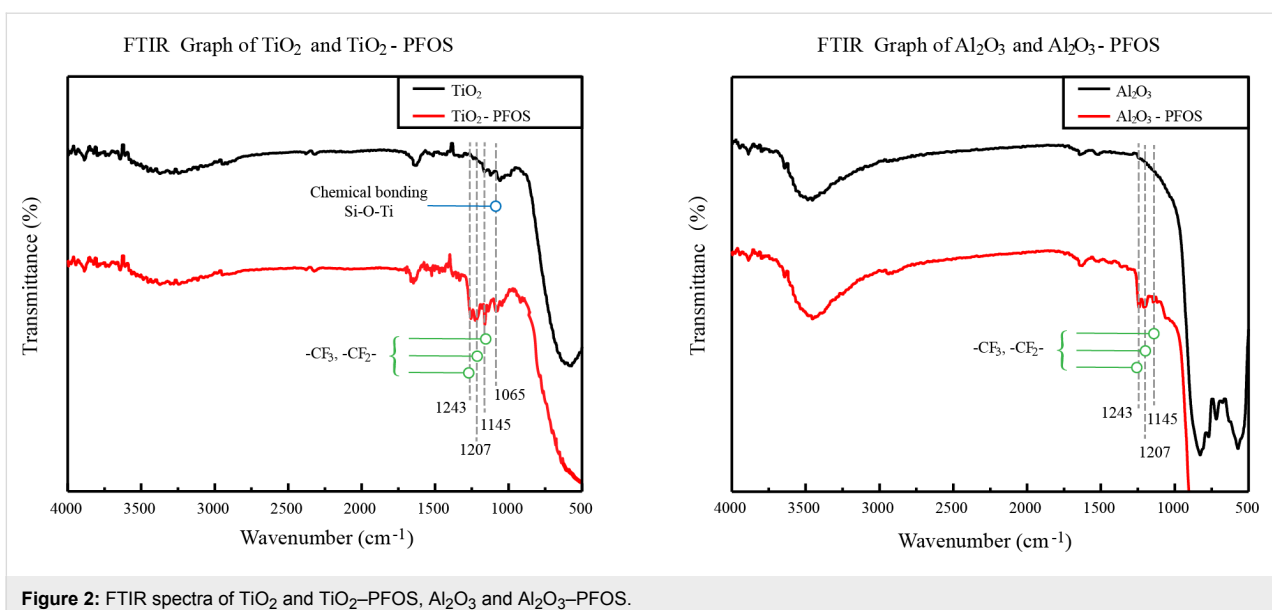


Figure 2: FTIR spectra of TiO_2 and TiO_2 -PFOS, Al_2O_3 and Al_2O_3 -PFOS.

in previous works [22–27]. The samples in the process of wettability switching were observed by FTIR, as shown in Figure 3a. For the TiO_2 -PFOS surface, as the UV exposure time increases, the peak intensity at 1629 cm^{-1} and 3436 cm^{-1} (assigned to the bending vibration and stretching vibration of $-\text{OH}$ groups, respectively) increased, while both peaks reduced after the heating treatment. At the same time, four peaks at 1207 cm^{-1} , 1243 cm^{-1} , 2850 cm^{-1} and 2919 cm^{-1} (attributed to the bending vibration and stretching vibration of $-\text{CF}_2-$ and $-\text{CF}_3$ groups) undergo no obvious changes either under UV illumination or high temperature exposure. The change in transmittance for selected transitions are listed in Figure 3b, which shows that the change of $-\text{OH}$ in TiO_2 is much larger than the change of $-\text{CF}_2-$ or $-\text{CF}_3$ in PFOS. The change of $-\text{CF}_2-$ or $-\text{CF}_3$ can be observed after long time UV illumination as shown in Figure 4. Finally, PFOS was completely removed due to UV illumination and the chemical bonding between TiO_2 and PFOS ($\text{Si}-\text{O}-\text{Ti}$) is without exception. The Al_2O_3 -PFOS samples achieved the transition to super-wettability under UV illumination but required a much longer time of up to 90 min. The bands at

1210 cm^{-1} and 1240 cm^{-1} which represent the vibration of the $-\text{CF}_2-$ and $-\text{CF}_3$ groups in PFOS was not recovered, while the $-\text{OH}$ vibration in Al_2O_3 experienced no significant change.

The wettability transition of TiO_2 under UV illumination and heat treatment has been previously reported and was explained by the formation of $\text{Ti}-\text{O}-\text{H}$ bonds under UV light, while heating of the surface results in the decrease in the concentration of $\text{Ti}-\text{O}-\text{H}$ bonds [33,34]. As reported, due to the low band gap energy of TiO_2 , the photo-induced electron-hole pairs are generated on the TiO_2 surfaces under UV illumination. The holes lead to the production of oxygen vacancies to enhance the adsorption of hydroxy groups, while the hydroxy groups are replaced by oxygen atoms that have a stronger bond on the defect sites during heating process. However, the change in TiO_2 cannot fully explain the fast wettability transition of the TiO_2 -PFOS coated surface. Based on the data shown in Figure 3 and Figure 4, the $-\text{CF}_2-$ and $-\text{CF}_3$ groups of PFOS were degraded and oxidized due to the high energy of UV illumination. The oxygen in the air stimulates a metastable state

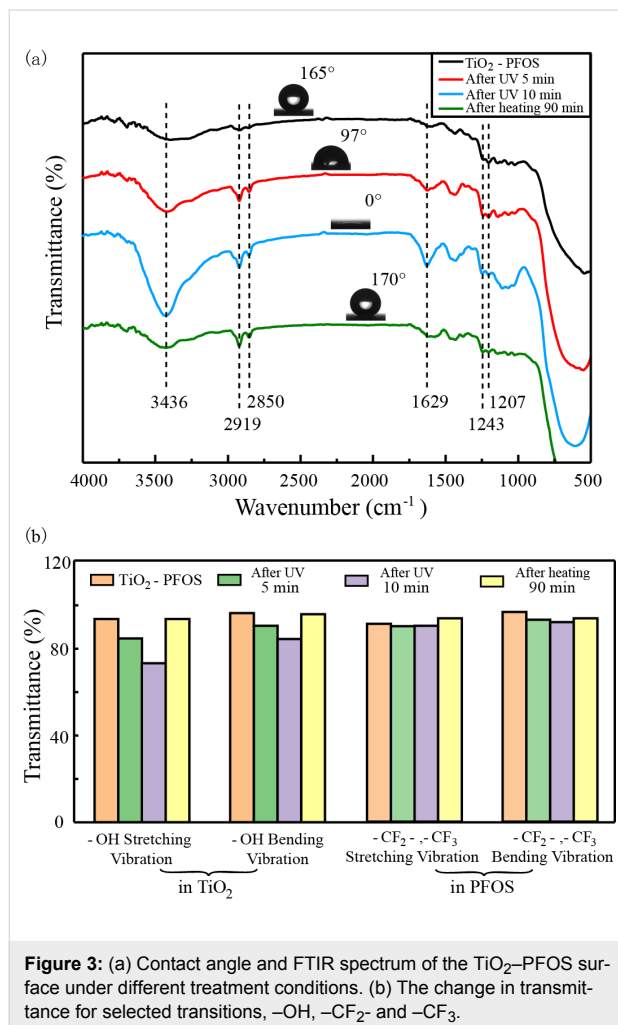


Figure 3: (a) Contact angle and FTIR spectrum of the TiO_2 -PFOS surface under different treatment conditions. (b) The change in transmittance for selected transitions, $-\text{OH}$, $-\text{CF}_2-$ and $-\text{CF}_3$.

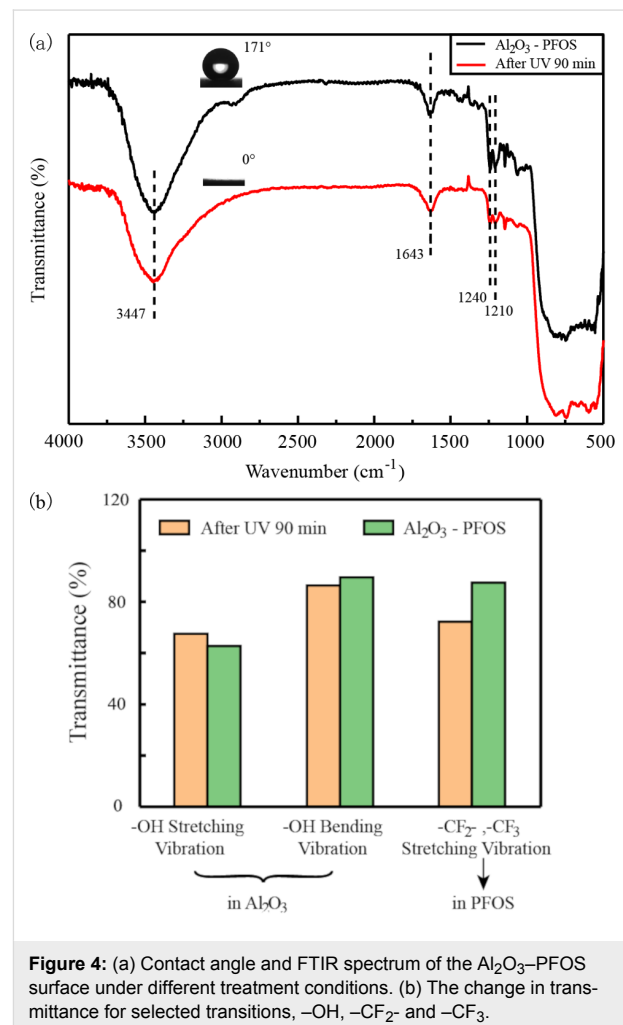


Figure 4: (a) Contact angle and FTIR spectrum of the Al_2O_3 -PFOS surface under different treatment conditions. (b) The change in transmittance for selected transitions, $-\text{OH}$, $-\text{CF}_2-$ and $-\text{CF}_3$.

which has a strong oxidizing property. In addition, the end of the fluorocarbon chains were changed into $-OH$ groups which could decrease the WCA faster with increasing UV illumination time. It can thus be inferred that the oxidation of PFOS is due to UV illumination and the photocatalytic effect of TiO_2 . Unlike the changes occurring in TiO_2 , unfortunately, this change in PFOS is not reversible. The mechanism for the wettability transition of the TiO_2 -PFOS coated surface under UV illumination and heating treatment is shown in Figure 5. Since the change in PFOS is not reversible, the wettability transition cycles cannot continue indefinitely, and the surface will remain superhydrophilic when most of the $-CF_2-$ and $-CF_3$ groups are replaced by the $-OH$ groups on PFOS. PFOS has a short carbon chain which can enhance the change of the $-CF_2-$ and $-CF_3$ groups and results in the much faster conversion time from superhydrophobicity to superhydrophilicity compared with the previous works [35,36]. The irreversible replacement of $-CF_2-$

and $-CF_3$ groups by $-OH$ groups on PFOS was also confirmed by the wettability transition of the Al_2O_3 -PFOS coated surfaces.

Limitation of switchable cycles

To further study the wettability switching of the surfaces, four samples comprised of a uniform weight of TiO_2 modified by different concentrations of PFOS were sprayed onto the glass samples. All the coated surfaces were initially superhydrophobic. Then the coated samples were placed under UV illumination until they transitioned to superhydrophilic, and were thereafter heated in an air-dry oven until they recovered their superhydrophobic property – this cycle was repeated until the surfaces could no longer recover the superhydrophobic property. For each concentration of PFOS, five identical samples were prepared for statistical reliability. The experimental results are shown in Table 1, where it can be seen that the number of

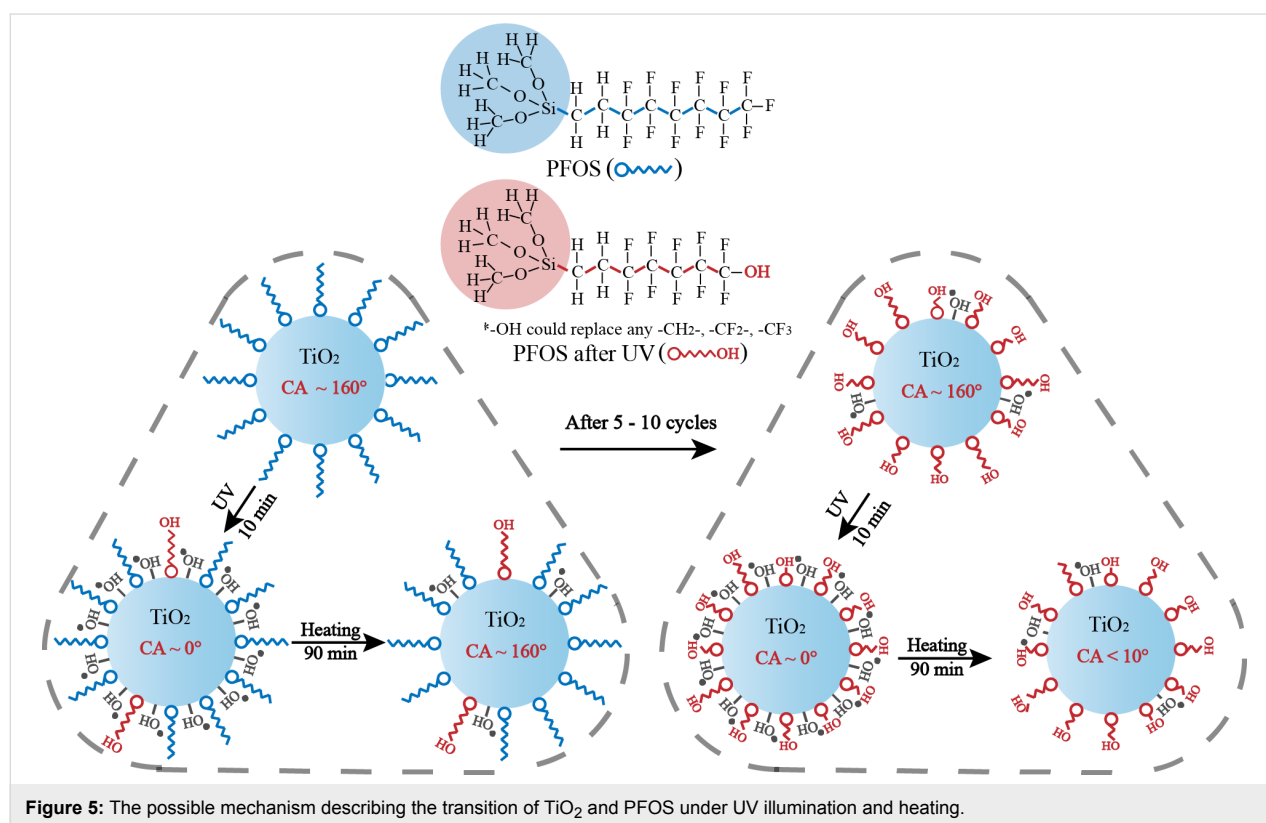


Figure 5: The possible mechanism describing the transition of TiO_2 and PFOS under UV illumination and heating.

Table 1: Effect of PFOS concentration on the wettability conversion time and number of conversion cycles.

Amount of PFOS in 50 mL ethanol (g)	Initial contact angle ($^\circ$)	R_a (μm)	Wettability conversion time (min)	Number of cycles
0.5	169	2.334	5	0–1
1.0	171	2.627	10	2–3
1.5	172	2.550	30	5–6
2.0	168	2.877	60	3–4

cycles first increases with the concentration of PFOS, then decreases, while the switching time from superhydrophobic to superhydrophilic increases constantly with increasing PFOS concentration. This phenomena indicates that more PFOS can provide more $-CF_2-$, $-CF_3$ and can initially increase the maximum number of conversion cycles. However, an excess of PFOS results in an increase in the time to achieve superhydrophilicity which enhances the amount of $-CF_2-$, $-CF_3$ changed in one cycle, and subsequently decreases the number of possible cycles. As a result, to obtain a faster wettability transition time as well as a larger number of conversion cycles, an appropriate amount of PFOS and TiO_2 is needed. It should be noted that with the same concentration of PFOS, the total UV illumination time for the surface to transition to unrecovered superhydrophilicity for TiO_2 -PFOS and Al_2O_3 -PFOS is 30 min and 90 min, respectively. This indicates that the oxidization time of PFOS is increased by the photocatalytic effect of TiO_2 .

For the sample with 1.5 g PFOS, the CA of the six cycles and the images of the conversion processes in the first and the last cycles are shown in Figure 6. The transition time from superhydrophobic to superhydrophilic decreased from the first cycle to the last cycle. This can be explained by the unrecoverable dissociation of the $-CF_2-$ and $-CF_3$ groups, which is also in agreement with the proposed mechanism in Figure 5.

Conclusion

TiO_2 nanoparticles modified with PFOS (which has relatively short carbon chains) were applied on glass substrates to achieve fast, switchable super-wettability, demonstrated by a WCA that could be recovered from $\approx 165^\circ$ to almost 0° . The experimental results show that the PFOS could reduce the conversion time from nearly 1 h to about 10 min, and the superhydrophobicity of the surfaces could be recovered after heating for 90 min at $120^\circ C$. However, it was shown that certain concentrations of PFOS limit the number of recovery cycles, whereby the optimal concentration of PFOS was identified to achieve about 5 to 10 cycles. The unrecoverable change of the $-CF_2-$ and $-CF_3$ groups on PFOS and the recoverable change of $-OH$ groups on TiO_2 were recorded by FTIR. These effects can explain both the shorter transition time and the limitation that (initially) the change of the $-CF_2-$ and $-CF_3$ groups leads to a quicker conversion time from superhydrophobicity to superhydrophilicity. However, this is only true when most of the $-CF_2-$ and $-CF_3$ groups are changed unrecoverably, and the whole surface cannot not transition back to a superhydrophobic state.

Experimental

Materials and chemicals

Titanium dioxide (TiO_2 , rutile) with a diameter of ≈ 25 nm and aluminium dioxide (Al_2O_3) with a diameter of ≈ 30 nm were

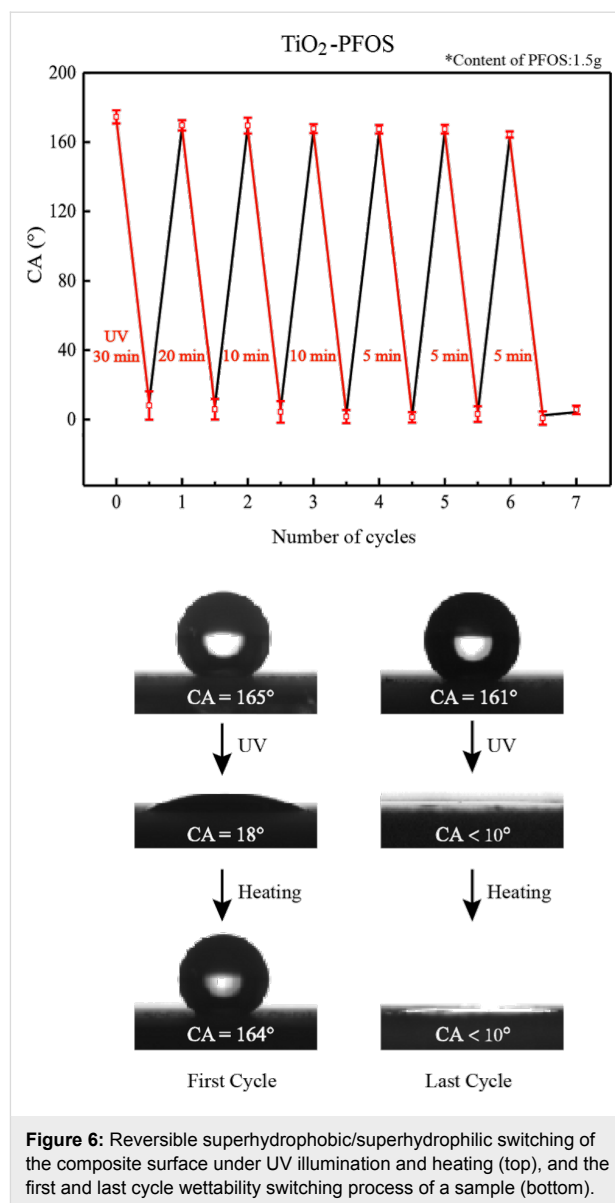


Figure 6: Reversible superhydrophobic/superhydrophilic switching of the composite surface under UV illumination and heating (top), and the first and last cycle wettability switching process of a sample (bottom).

acquired from Shanghai Aladdin Bio-Chem Technology Corporation (Shanghai, China). *1H,1H,2H,2H*-Perfluorooctyl-(trimethoxy)silane (PFOS) was obtained from Shanghai Macklin Biochemical Corporation (Shanghai, China). Other chemicals include 99.9% ethanol used as the solvent and de-ionized water was used in the CA measurements.

Preparation of coating surfaces

Rutile phase TiO_2 was modified by a simple hydrolysis reaction in order to obtain superhydrophobicity. In the modification process, 1 g of PFOS was dissolved into 50 mL ethanol and stirred for 1 h at ambient temperature in order to fully hydrolyse fluoroalkylsilane. Next, 3 g of rutile TiO_2 was added into the solution and stirred for another 1 h to form the suspension. The suspension could be used to spray or paint a substrate with a

spray gun (20 kPa). When the surfaces were dried, the superhydrophobicity is revealed. Al₂O₃ was modified by the same method as TiO₂.

UV illumination and heating experiments

A UV lamp (30 W) obtained from Cnlight Optical-Electrical Technology Corporation (Guangdong, China) was used to generate the UV illumination. The ultraviolet power density was set at 94 μW/cm² and the wavelength was 254 nm. The change of the WCA under UV light illumination was measured at short intervals. For the heating process, which was employed to recover the superhydrophobicity, the surface was heated in the air-dry oven at 150 °C for 90 min after UV illumination. The switching time from superhydrophilic to superhydrophobic was found to be reduced with increasing heating temperature.

Characterization

The microstructure of the coating surfaces was studied using scanning electron microscopy (SEM, ZEISS MERLIN Compact SEM, operated at a 20 kV acceleration voltage, Carl Zeiss Jena, Germany), and the surface roughness was measured with a laser confocal microscope (LCM, OLS5000, Olympus, Japan). The chemical modification and the end group changes on the surfaces was studied by Fourier transform infrared spectroscopy (FTIR, Nicolet iS50, Thermo Scientific, USA). The contact angles were measured at room temperature with an optical contact angle meter (DropMeter™ Element A-60, Maist, Ningbo, China), where the static CAs of the droplets (6 μL) placed onto the surfaces were measured five times at different locations.

Acknowledgements

This research was supported by the National Natural Science Foundation of China (Grant Nos. 51505108 and 51475118) and Key Laboratory of Micro-systems and Micro-structures Manufacturing of Ministry of Education, Harbin Institute of Technology (No. 2017KM009).

ORCID® IDs

Yunlu Pan - <https://orcid.org/0000-0003-1836-7751>

References

- Israelachvili, J. N. Adhesion, Friction and Lubrication of Molecularly Smooth Surfaces. In *Fundamentals of Friction: Macroscopic and Microscopic Processes*; Singer, I. L.; Pollock, H. M., Eds.; NATO ASI Series (Series E: Applied Sciences), Vol. 220; Springer Netherlands: Dordrecht, Netherlands, 1992. doi:10.1007/978-94-011-2811-7_19
- Bhushan, B. *Biomimetics*; Springer International Publishing: Cham, Switzerland, 2018. doi:10.1007/978-3-642-25408-6
- Sun, Z.; Liao, T.; Liu, K.; Jiang, L.; Kim, J. H.; Dou, S. X. *Small* **2014**, *10*, 3001–3006. doi:10.1002/sml.201400516
- Jin, X.; Shi, B.; Zheng, L.; Pei, X.; Zhang, X.; Sun, Z.; Du, Y.; Kim, J. H.; Wang, X.; Dou, S.; Liu, K.; Jiang, L. *Adv. Funct. Mater.* **2014**, *24*, 2721–2726. doi:10.1002/adfm.201304184
- Wang, Y.; Ma, K.; Xin, J. H. *Adv. Funct. Mater.* **2018**, *28*, 1705128. doi:10.1002/adfm.201705128
- Jeevanandam, J.; Barhoum, A.; Chan, Y. S.; Dufresne, A.; Danquah, M. K. *Beilstein J. Nanotechnol.* **2018**, *9*, 1050–1074. doi:10.3762/bjnano.9.98
- Li, F.; Wang, Z.; Huang, S.; Pan, Y.; Zhao, X. *Adv. Funct. Mater.* **2018**, *28*, 1706867. doi:10.1002/adfm.201706867
- Xu, Z.; Zhou, H.; Tan, S.; Jiang, X.; Wu, W.; Shi, J.; Chen, P. *Beilstein J. Nanotechnol.* **2018**, *9*, 508–519. doi:10.3762/bjnano.9.49
- Sun, Z.; Liao, T.; Liu, K.; Jiang, L.; Kim, J. H.; Dou, S. X. *Nano Res.* **2013**, *6*, 726–735. doi:10.1007/s12274-013-0350-6
- Bhushan, B., Ed. *Springer Handbook of Nanotechnology*; Springer Handbooks; Springer Berlin: Berlin, Germany, 2017. doi:10.1007/978-3-662-54357-3
- Liang, C.; Wen, J.; Liao, X. *Beilstein J. Nanotechnol.* **2018**, *9*, 1793–1801. doi:10.3762/bjnano.9.170
- Dalei, J.; Shiyu, S.; Lei, H. *Int. J. Heat Mass Transfer* **2018**, *128*, 1344–1350. doi:10.1016/j.ijheatmasstransfer.2018.08.006
- Khongtong, S.; Ferguson, G. S. *Langmuir* **2004**, *20*, 9992–10000. doi:10.1021/la0497191
- Muthiah, P.; Boyle, T. J.; Sigmund, W. *Macromol. Mater. Eng.* **2013**, *298*, 1251–1258. doi:10.1002/mame.201200411
- Zhu, L.; Xu, J.; Xiu, Y.; Sun, Y.; Hess, D. W.; Wong, C.-P. *J. Phys. Chem. B* **2006**, *110*, 15945–15950. doi:10.1021/jp063265u
- Zhang, G.; Duan, Z.; Wang, Q.; Li, L.; Yao, W.; Liu, C. *Appl. Surf. Sci.* **2018**, *427*, 628–635. doi:10.1016/j.apsusc.2017.08.082
- Fujishima, A.; Zhang, X.; Tryk, D. A. *Surf. Sci. Rep.* **2008**, *63*, 515–582. doi:10.1016/j.surfrep.2008.10.001
- Li, W.; Guo, T.; Meng, T.; Huang, Y.; Li, X.; Yan, W.; Wang, S.; Li, X. *Appl. Surf. Sci.* **2013**, *283*, 12–18. doi:10.1016/j.apsusc.2013.05.085
- Awaja, F.; Gilbert, M.; Kelly, G.; Fox, B.; Pigram, P. J. *Prog. Polym. Sci.* **2009**, *34*, 948–968. doi:10.1016/j.progpolymsci.2009.04.007
- Lai, Y.; Huang, J.; Cui, Z.; Ge, M.; Zhang, K.-Q.; Chen, Z.; Chi, L. *Small* **2016**, *12*, 2203–2224. doi:10.1002/sml.201501837
- Wang, R.; Hashimoto, K.; Fujishima, A.; Chikuni, M.; Kojima, E.; Kitamura, A.; Shimohigoshi, M.; Watanabe, T. *Nature* **1997**, *388*, 431–432. doi:10.1038/41233
- Jin, C.; Yan, R.; Huang, J. *J. Mater. Chem.* **2011**, *21*, 17519–17525. doi:10.1039/c1jm13399c
- Chagas, G. R.; Weibel, D. E. *Polym. Bull.* **2017**, *74*, 1965–1978. doi:10.1007/s00289-016-1817-x
- Villafiorita Monteleone, F.; Caputo, G.; Canale, C.; Cozzoli, P. D.; Cingolani, R.; Fragouli, D.; Athanassiou, A. *Langmuir* **2010**, *26*, 18557–18563. doi:10.1021/la1026398
- Ding, X.; Zhou, S.; Gu, G.; Wu, L. *J. Mater. Chem.* **2011**, *21*, 6161–6164. doi:10.1039/c0jm04546b
- Kong, Y.; Liu, Y.; Xin, J. H. *J. Mater. Chem.* **2011**, *21*, 17978–17987. doi:10.1039/c1jm12516h
- Sun, T.; Wang, G.; Feng, L.; Liu, B.; Ma, Y.; Jiang, L.; Zhu, D. *Angew. Chem., Int. Ed.* **2004**, *43*, 357–360. doi:10.1002/anie.200352565
- Sawada, E.; Kakehi, H.; Chounan, Y.; Miura, M.; Sato, Y.; Isu, N.; Sawada, H. *Composites, Part B* **2010**, *41*, 498–502. doi:10.1016/j.compositesb.2010.04.002
- Petroffe, G.; Wang, C.; Sallenave, X.; Sini, G.; Goubard, F.; Peralta, S. *J. Mater. Chem. A* **2015**, *3*, 11533–11542. doi:10.1039/c5ta01710f

30. Qing, Y.; Yang, C.; Yu, N.; Shang, Y.; Sun, Y.; Wang, L.; Liu, C. *Chem. Eng. J.* **2016**, *290*, 37–44. doi:10.1016/j.cej.2016.01.013
31. Ito, Y.; Heydari, M.; Hashimoto, A.; Konno, T.; Hirasawa, A.; Hori, S.; Kurita, K.; Nakajima, A. *Langmuir* **2007**, *23*, 1845–1850. doi:10.1021/la0624992
32. Liu, C. S.; Zheng, D. M.; Zhou, J. G.; Wan, Y.; Li, Z. W. *Mater. Sci. Forum* **2011**, *688*, 102–106. doi:10.4028/www.scientific.net/msf.688.102
33. Kumar, S. G.; Devi, L. G. *J. Phys. Chem. A* **2011**, *115*, 13211–13241. doi:10.1021/jp204364a
34. Nakata, K.; Fujishima, A. *J. Photochem. Photobiol., C* **2012**, *13*, 169–189. doi:10.1016/j.jphotochemrev.2012.06.001
35. Sugimura, H.; Ushiyama, K.; Hozumi, A.; Takai, O. *Langmuir* **2000**, *16*, 885–888. doi:10.1021/la990953e
36. Hou, W.; Wang, Q. *Langmuir* **2009**, *25*, 6875–6879. doi:10.1021/la900151y

License and Terms

This is an Open Access article under the terms of the Creative Commons Attribution License (<http://creativecommons.org/licenses/by/4.0>). Please note that the reuse, redistribution and reproduction in particular requires that the authors and source are credited.

The license is subject to the *Beilstein Journal of Nanotechnology* terms and conditions: (<https://www.beilstein-journals.org/bjnano>)

The definitive version of this article is the electronic one which can be found at:
[doi:10.3762/bjnano.10.87](https://doi.org/10.3762/bjnano.10.87)